Microgravity Sci. Technol manuscript No.
(will be inserted by the editor)

Effect of gravity forces on heat transfer and pressure drop during condensation of R134a

Stephane Lips · Josua P. Meyer

Received: date / Accepted: date

Abstract The present paper is dedicated to an experimental study of the effect of gravity forces during condensation of R134a in an 8.38 mm inner diameter smooth tube in inclined orientations. Flow pattern, heat transfer coefficient and pressure drop are presented as a function of the inclination angle for different mass fluxes ($G = 200-400$ kg/m^{2}s) and different vapour qualities ($x = 0.1-0.9$). An apparent void fraction was also defined from the pressure drop measurements. Maps of the inclination effect on the flow pattern, heat transfer coefficient and apparent void fraction were drawn and a limit between the gravity-dependent and gravity-non-dependent zone was determined for each case. It was shown that the flow can be considered as gravity-non-dependent for high mass fluxes ($G \geq 300$ kg/m^{2}s) and high vapour qualities ($x > 0.6-0.7$).

Keywords Condensation · Gravity forces · Flow pattern · Heat transfer coefficient · Pressure drop · Void fraction

1 Introduction

The effect of gravity forces and more generally of acceleration forces on a system can be studied through three different approaches: experiments can be done under microgravity conditions (e.g. during parabolic flights), under enhanced gravity conditions (e.g. in centrifuges) or under normal gravity conditions, but with changing the orientation of the system compared with the gravity direction. The present study focuses on the third approach to study the effect of gravity forces on the properties of a condensing flow in a smooth tube. Convective condensation inside smooth and enhanced tubes in horizontal orientation and in normal gravity condition has been widely studied during the last years (Liebenberg and Meyer, 2008). Several accurate predictive tools have been developed, in order to determine the flow pattern map (El Hajal et al., 2003), the heat transfer coefficient (Thome et al., 2003; Cavallini et al., 2006) and the pressure drop (Moreno Quibén and Thome, 2007). Models have been tested with a wide range of fluids and experimental conditions. Most of the time, the gravitational forces are taken into account by means of empirical or semi-empirical correlations. No complete mechanistic model exists for the whole range of flow patterns, vapour quality and mass flow and the results of existing models cannot be extrapolated to microgravity conditions.

Some studies dealing with two-phase flows in inclined tubes are available in the literature. This kind of study can be useful to get a better understanding of the gravitational effects on the flow properties. However, only a few of the studies considered the whole range of inclination angles, from vertical downward to vertical upward flow. Barnea (1987) proposed a model of flow pattern map for the whole range of inclination angles. Spedding et al. (1982) conducted an intensive study of two-phase pressure drops in inclined tubes and Beggs and Brill (1973) proposed a correlation to predict the void fraction for all inclination angles. All of these studies have been conducted with air as the vapour phase and most of the time water as the liquid phase. Thus, extrapolations of the results to applications using refrigerant are uncertain. Studies of condensation in inclined tubes are very rare (Wang et al., 1998; Würfel et al., 2003; Akhavan-Behabadi et al., 2007) and are limited to very specific experimental conditions (Lips and Meyer, 2011c) .

The present paper aims to give a better understanding of the effect of the gravitational forces on the flow properties: the flow pattern, the heat transfer coefficient and the pressure drop are experimentally studied as a function of the incli-

S. Lips · J.P. Meyer (✉)
Department of Mechanical and Aeronautical Engineering, University of Pretoria, Private Bag X20, Hatfield, 0028, South Africa
E-mail: josua.meyer@up.ac.za

nation angle for different mass fluxes and different vapour qualities. For each property, a limit is defined between a gravity-dependent and a gravity-non-dependent zone.

2 Experimental set-up and procedure

The experimental facility used in this study was already presented in previous works (Lips and Meyer, 2011a,b), and is therefore only briefly described. The set-up consisted of a vapour-compression cycle circulating the refrigerant R134a with two high-pressure condensation lines: the test line and the bypass line (Fig. 1). The bypass line was used to control the mass flow through the test line and the test pressure and temperature. The test line consisted of three water-cooled condensers: a pre-condenser, to control the inlet vapour quality, the test condenser, where the measurements were performed, and the post-condenser, to ensure that the fluid is fully liquid before the expansion valve (EEV). After the EEVs, the lines combined and entered a water-heated evapourator, followed by a suction accumulator and a scroll compressor. The test condenser consisted of a tube-in-tube counterflow heat exchanger, with water in the annulus and refrigerant on the inside. Its length was 1 488 mm and the inside channel was a copper tube with an inner diameter of 8.38 mm. Cylindrical sight glasses were positioned at the inlet and the outlet of the test condenser. It permitted flow visualisation and acted as insulators against axial heat conduction. Absolute pressures at the inlet and the outlet of the test condenser were measured by means of Gems Sensor pressure transducers and the pressure drop in the test condenser was measured by means of a FP2000 Sensotec differential pressure transducer. The length between the pressure taps for the differential pressure sensor was 1 702 mm. The pressure lines were heated by means of a heating wire and their temperatures were controlled by means of four thermocouples and a labview program to ensure that the refrigerant always stayed in the form of vapour in the lines. Straight calming sections of lengths 500 mm and 400 mm were positioned before and after the sight glasses respectively. At the inlet of the test section, the flow is supposed to be hydrodynamically developed whatever the inclination angle (Cho and Tae, 2001). The test section could be inclined from 90° upwards to 90° downwards by using flexible hoses at the inlet and the outlet of the test section. The outer-wall temperature of the inner tube of the test section was measured at seven stations equally spaced. The refrigerant temperature was taken at four stations: inlet and outlet of the test section, inlet of pre-condenser and outlet of the post-condenser. On the water side, the water temperature was measured at the inlet and the outlet of the pre-, test (i.e. test section) and post-condenser. The refrigerant and water mass flows through the pre-, test and post-condensers were measured with coriolis mass flow meters.

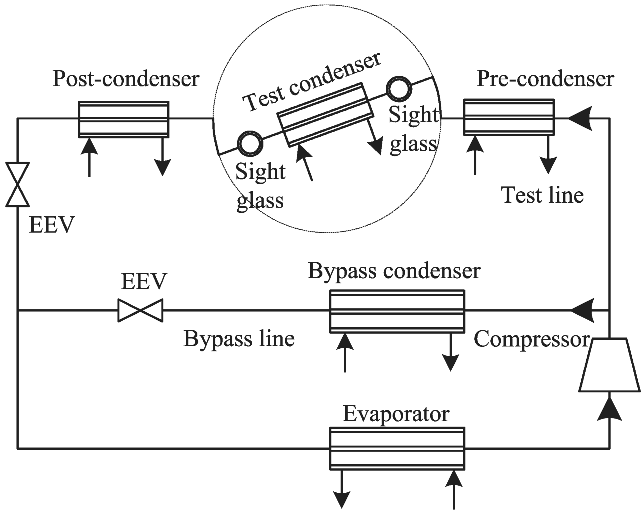

Fig. 1 Scheme of the experimental set-up

The instrumentation of the test section allowed the calculation of the energy balance from the inlet of the pre-condenser, where the fluid is fully vaporised, to the outlet of the post-condenser, where the fluid is fully liquid. The energy balance is defined as the percentage of heat that is lost, or gained, during the heat transfer between the water and the refrigerant in the three condensers. All the experiments were performed with an energy balance lower than 3%. A good energy balance allows the accurate determination of the inlet and outlet vapour qualities with the method presented in Suliman et al. (2009).

The heat transfer coefficient, α_{cond}, was calculated with the heat flux in the test condenser, $\dot{Q}_{test}$, measured on the

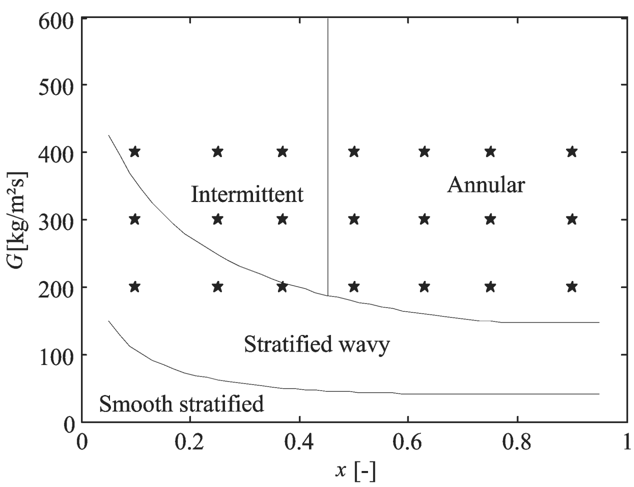

Fig. 2 Experimental data points plotted on the Thome-El Hajal flow pattern map (El Hajal et al., 2003)

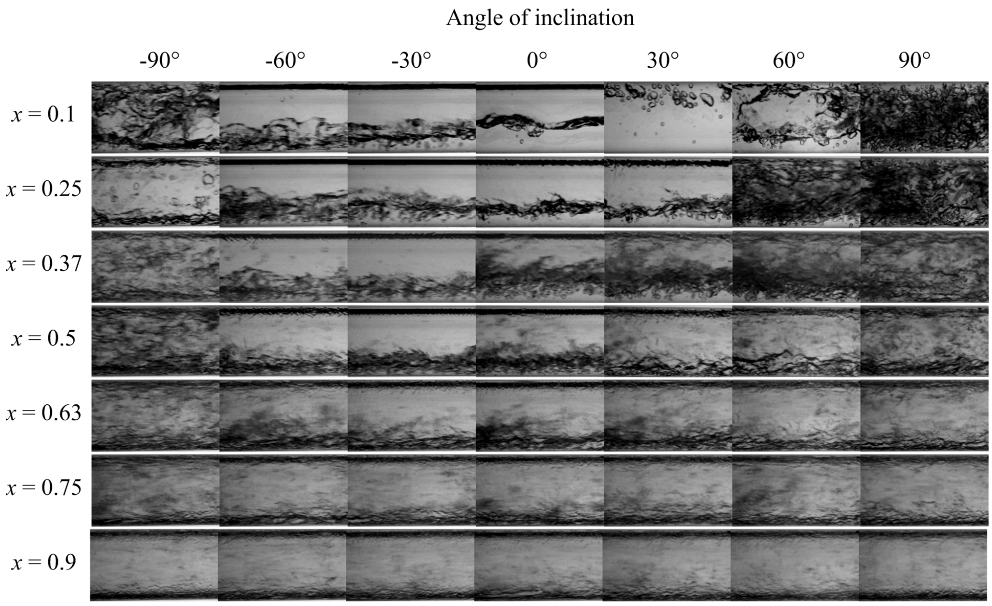

Fig. 3 Visualization of the flow ($G = 300$ kg/m^{2}s)

water side, and the difference between the average wall temperature, $\overline{T_{w,i}}$, and the saturation fluid temperature, T_{sat}:

$$\alpha_{cond} = \left| \frac{\dot{Q}_{test}}{A(\overline{T_{w,i}} - T_{sat})} \right| \quad (1)$$

A is the area of the internal surface of the inner tube. The average wall temperature is calculated by means of a trapezoidal numerical integration of the wall temperature measurements. More details about the post-processing of the data are available in Lips and Meyer (2011a,b).

In inclined orientation, the pressure drop measured by the differential pressure transducer must be corrected by taking into account the gravitational pressure difference in the lines between the sensor and the pressure taps:

$$\Delta P_{test} = \Delta P_{measured} + \Delta P_{lines} \quad (2)$$

As the refrigerant is fully vapourised in the lines, ΔP_{lines} can be depicted as:

$$\Delta P_{lines} = \rho_v g L_{\Delta P} \sin(\beta) \quad (3)$$

β is the inclination angle. In the present paper, $\beta > 0$ corresponds to an upward flow and $\beta < 0$ to a downward flow. The experiments were conducted for different mass fluxes G, vapour qualities x and inclination angles α. The average saturation temperature was kept constant at 40°C and for all the experiments, the heat transfer rate in the test condenser was equal to 200 W. This heat transfer rate led to a vapour quality difference across the test condenser between 0.11 and 0.055 depending on the mass flux. Fig. 2 summarises the experimental conditions on the Thome-El Hajal flow pattern map (El Hajal et al., 2003), drawn for condensing flow of R134a with a saturation temperature of 40°C in a horizontal tube with an inner diameter of 8.38 mm. For a horizontal orientation, the experimental conditions mainly correspond to intermittent and annular flow patterns at the boundary of the stratified flow.

3 Experimental Results

3.1 Flow patterns

In two-phase flows, the flow pattern is an important parameter as the distribution of the liquid and the vapour phases directly affects the heat transfer coefficients and the pressure drops. During the present study, the flow was recorded for each experimental condition by means of a high-speed camera, placed at the exit sight glass. The flow pattern was then determined visually. To simplify the study, only three types of flow patterns were considered: annular, stratified and intermittent. Annular flow occurs when the liquid is distributed around the circumference of the tube. The flow is stratified if most of the liquid is located at the bottom of the tube with only a thin liquid film at the top of the tube. Lastly, intermittent flows regroup the plug and slug flow, where liquid plugs alternate with vapour slugs, and churn flow, which is observed for near vertical orientations and consists of a highly chaotic flow where liquid plugs collapse in a central vapour core because of the gravitational forces. The transitions between the different flow patterns are continuous and thus some parameters were chosen by the authors. The transition from stratified to annular flow was supposed to occur when waves appeared on the liquid film at the top of the tube, denoting a thick liquid film mainly driven by shear forces. The transition to intermittent flow was supposed to occur when the waves touch the top of the tube.

Fig. 3 is an example of flow visualisation: photographs of the flow are presented for different inclination angles and different vapour qualities for a mass flux of 300 kg/m^{2}s. For high vapour qualities, the flow remains annular, whatever the inclination angle. For low vapour qualities, the flow can be either annular, stratified or intermittent depending on the inclination angle. It has been shown in a previous paper (Lips and Meyer, 2011a) that the same observation is valid for high and low mass fluxes as well: a high mass flux leads to an annular flow pattern whereas the flow pattern with a low mass flux depends on the inclination angle.

From these observations, it is possible to draw a map of the inclination effect on the flow pattern: in Fig. 4 are plotted the different types of flow patterns (represented by the circles, diamonds and triangles), which can be encountered for each experimental condition (represented by the black dots) depending on the inclination angle. For example, for $G = 300$ kg/m^{2}s and $x = 0.9$, the flow remains annular whatever the inclination angle. For $G = 300$ kg/m^{2}s and $x = 0.25$, the flow can be either stratified, annular and intermittent depending on the inclination angle and for $G = 300$ kg/m^{2}s and $x = 0.1$, only stratified and intermittent flows can be encountered. Fig. 4 shows that it is possible to make the distinction between two zones: a gravity-dependent zone, for low mass fluxes and/or low vapour qualities, where the flow pattern depends on the inclination angle, and a gravity-non-dependent zone, for high mass fluxes and high vapour qualities, where the flow pattern remains annular, whatever the inclination angle. In this zone, we can expect the properties of the flow to remain constant, whatever the orientation, as the shear forces are dominant compared with the gravitational and capillary forces. However, it is important to check this assumption experimentally in terms of heat transfer coefficients and pressure drops.

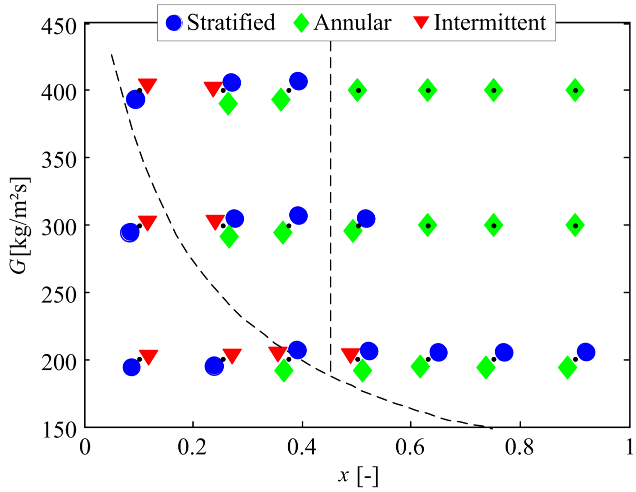

Fig. 4 Map of the inclination effect on the flow pattern. The markers represent the flow patterns that can be encountered depending on the inclination angle. The black dots represent the actual values of the mass fluxes and vapour qualities. Dashed lines represent the Thome-El Hajal flow pattern map (El Hajal et al., 2003), valid for the horizontal orientation

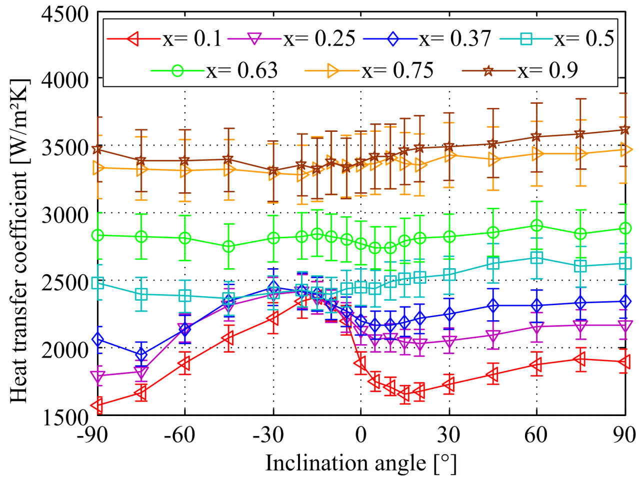

Fig. 5 Heat transfer coefficient versus inclination angle for different vapour qualities ($G = 300$ kg/m^{2}s)

3.2 Heat transfer coefficients

If the inclination angle affects the flow pattern, it also affects the heat transfer coefficient as it changes the circumferential liquid thickness, which corresponds to the main thermal resistance during a condensation process. Fig. 5 is an example of the heat transfer coefficient as a function of the inclination angle for different vapour qualities and for a mass flux of 300 kg/m^{2}s. The error bars correspond to the uncertainties of the measurements and are calculated thanks to the theory of the propagation of the errors. The resulting relative uncertainty of the heat transfer coefficient is between 6 and 10%. The heat transfer coefficient increases when the vapour quality increases. For high vapour qualities, it remains sensibly constant, whatever the tube orientation, whereas for low vapour qualities, the heat transfer coefficient is strongly affected by the inclination angle. For downward flows ($\beta < 0$), there is an optimal inclination angle, about -15°, which leads to the highest heat transfer coefficient. This angle corresponds to a stratified flow with the best trade-off between a low depth of the liquid at the bottom of the tube and a thin falling liquid film at the top of the tube. For upward flows ($\beta > 0$), an angle of 15° leads to a minimum heat transfer coefficient because of the occurrence of a plug and slug flow, with a liquid and vapour distribution that leads to a high thermal resistance.

The impact of the gravitational forces on the heat transfer coefficient can be summarised by the inclination effect I_α, defined as:

$$I_\alpha(G,x) = \left.\frac{\alpha_{cond,max} - \alpha_{cond,min}}{\alpha_{cond,\beta=0^\circ}}\right|_{G,x} \tag{4}$$

where $\alpha_{cond,max}$ and $\alpha_{cond,min}$ are the maximum and minimum heat transfer coefficients obtained for a specific mass flux and a specific vapour quality for all the inclination an-

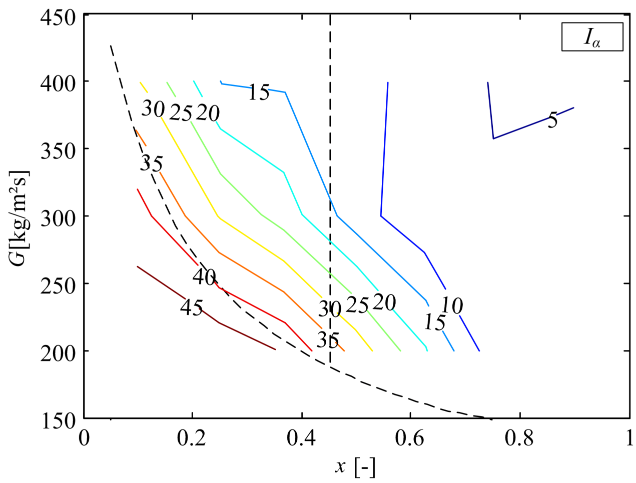

Fig. 6 Map of the inclination effect on heat transfer coefficient

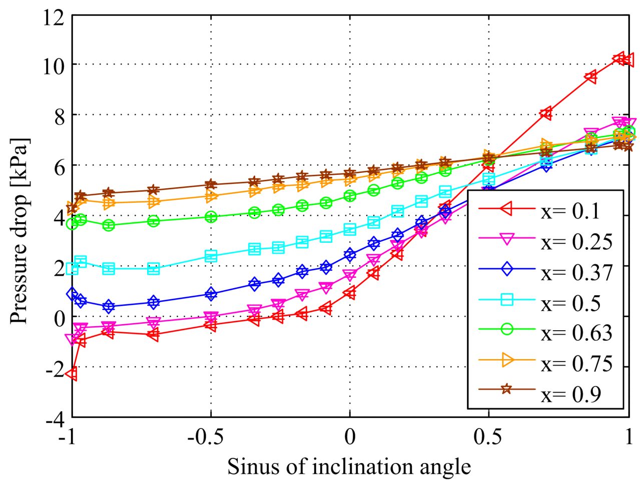

Fig. 7 Inclination effect on the pressure drops ($G = 300$ kg/m^{2}s)

gles. $\alpha_{cond,\beta=0^\circ}$ is the heat transfer coefficient obtained for the horizontal orientation in the same experimental conditions. By calculating I_α for all the experimental conditions, it is possible to draw a map of the inclination effect on the heat transfer coefficient: Fig. 6 represents the contours of the evolution of I_α with the vapour quality and the mass flux. This graph is plotted by means of a linear interpolation between all the data points summarised in Fig. 2.

The inclination effect on the heat transfer coefficient increases when the mass flux and the vapour quality decrease. For high mass fluxes, the inclination angle is in the order of magnitude of the measurement uncertainties (about 10%) and thus this zone can be considered as a gravity-non-dependent zone. It corresponds more or less to the gravity-non-dependent zone in terms of flow patterns in Fig. 4, where the flow remains annular whatever the tube orientation.

3.3 Pressure drops

An important issue in the design of condensers is the determination of the pressure drops during the condensation. The total pressure drop is actually the sum of three different terms: the momentum, the frictional and the gravitational pressure drops.

$$\Delta P_{test} = \Delta P_{mom} + \Delta P_{fric} + \Delta P_{grav} \tag{5}$$

The momentum pressure drop is due to the difference of kinetic energy between the outlet and the inlet of the tube. It depends on the evolution of the void fraction and the vapour quality along the tube. In the condition of the present study, it represents less than 10% of the total pressure drop and is estimated using Steiner's (Steiner, 1993) version of the Rouhani and Axelsson (Rouhani and Axelsson, 1970) correlation for the void fraction. In this article, the estimation of the momentum pressure drop is subtracted from the total pressure drop and the results are given in terms of the sum of the gravitational and frictional pressure drops only.

The frictional pressure drop is due to the shear stress between the liquid, the vapour and the wall. The gravitational pressure drop is due to the gravitational forces that act on the fluids. Its importance is proportional to the sinus of the inclination angle and to the apparent density of the flow, which depends on the void fraction:

$$\Delta P_{grav} = \rho_{eq} g L_{\Delta P} \sin(\beta) \tag{6}$$

with:

$$\rho_{eq} = \rho_l (1-\varepsilon) + \rho_v \varepsilon \tag{7}$$

L_{DP} is the length between the pressure taps.

Fig. 7 represents the pressure drop (corrected by the momentum pressure drop) as a function of the sinus of the inclination angle for different vapour qualities and a mass flux equal to 300 kg/m^{2}s. For a horizontal orientation, the pressure drop increases when the vapour quality increases. The pressure drop also increases when the inclination angle increases, because of the increase of the gravitational pressure drop. Note that without an accurate knowledge of the void fraction, it is not possible to make the distinction between the frictional and the gravitational pressure drops. However, it has been shown in Lips and Meyer (2011b) that it is possible to define an apparent gravitational pressure drop, ΔP^*_{grav}, as the difference between the measured pressure drop and the pressure drop obtained for the same mass flux and vapour quality in horizontal orientation:

$$\Delta P^*_{grav} = \Delta P_{test} - \Delta P_{test,\beta=0^\circ} \tag{8}$$

The apparent gravitational pressure drop is equal to the actual gravitational pressure drop only if the frictional pressure drop does not depend on the inclination angle. From the apparent gravitational pressure drop, it is also possible to define an apparent void fraction ε^* by means of the equations 6

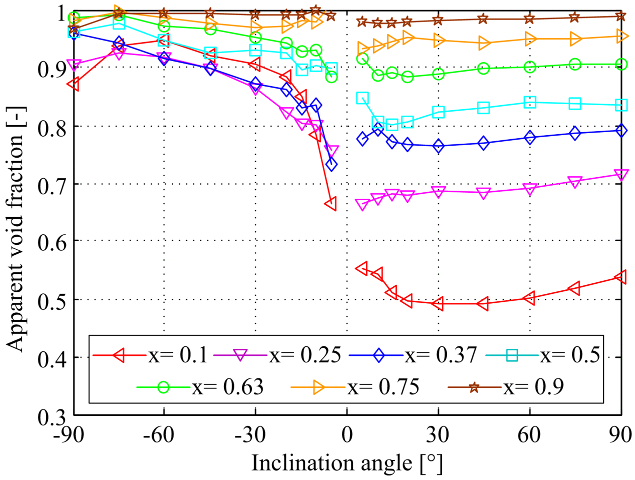

Fig. 8 Inclination effect on the apparent void fraction ($G = 300$ kg/m^{2}s)

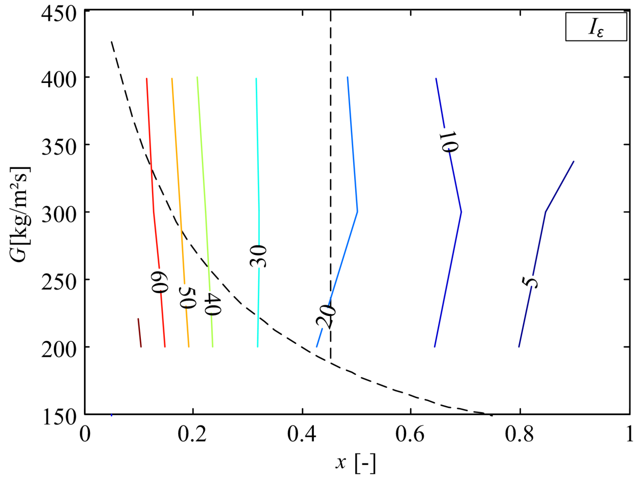

Fig. 9 Map of the inclination effect on the apparent void fraction

and 7, using the apparent gravitational pressure drop instead of the actual gravitational pressure drop. Fig. 8 represents the apparent void fraction as a function of the inclination angle for different vapour qualities and a mass flux equal to 300 kg/m^{2}s. The apparent void fraction decreases when the inclination increases because of the increase of the slip ratio between the phases due to the gravitational forces that mainly act on the liquid phase. The apparent void fraction is equal to the actual void fraction only if the frictional pressure drop variation is small compared to the gravitational pressure drop variation. However, the apparent void fraction can always be used as a physical parameter to study the inclination effect on the pressure drop. Assimilating the apparent void fraction to the actual void fraction must be done very carefully even if the two parameters probably follow the same trends in most of the cases.

As we defined an inclination effect on the heat transfer coefficient I_α, we can define an inclination effect on the apparent void fraction I_ε. It can be depicted as the difference between the maximum and minimum apparent void fraction, divided by the average of the apparent void fraction, for a specific mass flux and a specific vapour quality for all the inclination angles:

$$I_\varepsilon(G,x) = \left.\frac{\varepsilon^*_{max} - \varepsilon^*_{min}}{\overline{\varepsilon^*}}\right|_{G,x} \tag{9}$$

Note that the denominator is not the apparent void fraction for the horizontal orientation as ε^* is not defined for $\beta = 0°$.

Fig. 9 represents a map of the inclination effect on the apparent void fraction. The inclination effect decreases when the vapour quality increases but it seems to be independent of the mass flux. As for the map of the inclination effect on the heat transfer coefficient, it is possible to draw a limit between gravity-dependent and non-dependent zones for $I_\varepsilon = 10\%$.

So far, we have presented the inclination effect on the flow pattern, the heat transfer coefficient and the apparent void fraction. These three criteria allow the determination of gravity-dependent and non-dependent zones. Fig. 10 summarises the limits presented for each criterion with dashed lines. The black stars represent the position of the experimental conditions. The different limits are in a relatively good agreement considering the uncertainty of the inclination effect on the heat transfer coefficients and apparent void fractions. For high vapour qualities ($x > 0.6 - 0.7$) and high mass fluxes ($G \geq 300$ kg/m^{2}s), the flow properties are independent of the inclination angle. We can deduce that the gravitational forces are negligible in these conditions, compared with the shear forces. For lower mass fluxes and lower vapour qualities, the flow properties depend on the inclination angle and specific studies and models have to be developed to predict the flow pattern, the heat transfer coefficient and the pressure drop depending on the tube orientation.

4 Conclusions

An experimental study on convective condensation of R134a in an inclined tube was conducted. Mass fluxes in the range of 200-400 kg/m^{2}s and vapour qualities in the range of 0.1-0.9 were tested for inclination angles from vertical downward to vertical upward orientations. The effects of the gravity forces on the flow pattern, heat transfer coefficient, pressure drop and apparent void fraction were highlighted and the limits between the gravity-dependent and gravity-non-dependent flows were determined. The three criteria chosen for this limit were in a good agreement with each other: the flow can be considered as gravity-non-dependent for high mass fluxes ($G \geq 300$ kg/m^{2}s) and high vapour qualities ($x > 0.6 - 0.7$). In these conditions, the existing correlations can be used whatever the inclination angle and for both

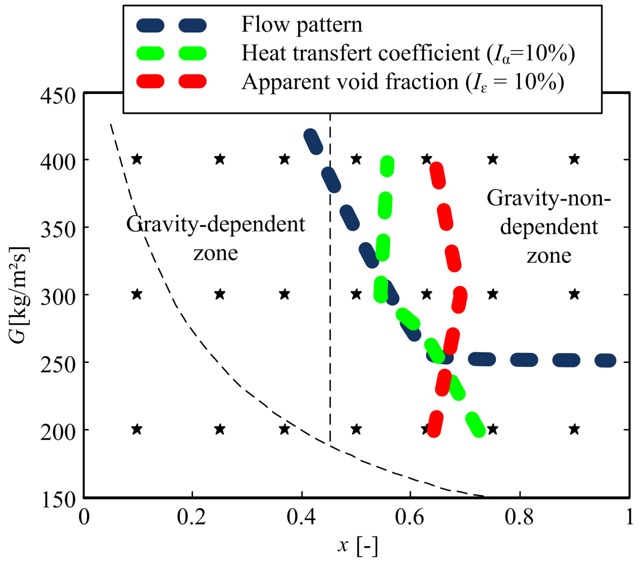

Fig. 10 Summarised map of the gravity-dependent limits

normal-gravity and microgravity conditions. For lower mass fluxes and/or lower vapour qualities, the flow properties depend on the gravitational forces and specific models and correlations have to be developed to predict the flow pattern, heat transfer coefficient and pressure drop for inclined orientations and/or in microgravity conditions. As a perspective, it would be interesting to extend the inclination effect maps for higher mass fluxes in order to determine the upper limit of the gravity-dependent zone in terms of mass flux. It would also be interesting to draw such maps for increased gravity conditions.

Acknowledgements The funding obtained from the NRF, TESP, University of Stellenbosch/University of Pretoria, SANERI/SANEDI, CSIR, EEDSM Hub and NAC is acknowledged and duly appreciated.

References

Akhavan-Behabadi, M. A., Kumar, R., Mohseni, S. G.: Condensation heat transfer of R-134a inside a microfin tube with different tube inclinations. International Journal of Heat and Mass Transfer **50**(23-24), 4864 (2007)

Barnea, D.: A unified model for predicting flow-pattern transitions for the whole range of pipe inclinations. International Journal of Multiphase Flow **13**(1), 1 (1987)

Beggs, D. H., Brill, J. P.: A study of two-phase flow in inclined pipes. Journal of Petroleum Technology **25**(5) (1973)

Cavallini, A., Col, D. D., Doretti, L., Matkovic, M., Rossetto, L., Zilio, C., Censi, G.: Condensation in horizontal smooth tubes: a new heat transfer model for heat exchanger design. Heat Transfer Engineering **27**(8), 31 (2006)

Cho, K., Tae, S.: Condensation heat transfer for R-22 and R-407C refrigerant-oil mixtures in a microfin tube with a U-bend. International Journal of Heat and Mass Transfer **44**, 2043 (2001)

El Hajal, J., Thome, J. R., Cavallini, A.: Condensation in horizontal tubes. Part 1: two-phase flow pattern map. International Journal of Heat and Mass Transfer **46**(18), 3349 (2003)

Liebenberg, L., Meyer, J. P.: A review of flow pattern-based predictive correlations during refrigerant condensation in horizontally smooth and enhanced tubes. Heat Transfer Engineering **29**(1), 3 (2008)

Lips, S., Meyer, J. P.: Experimental study of convective condensation in an inclined smooth tube. Part I: Inclination effect on flow pattern and heat transfer coefficient. International Journal of Heat and Mass Transfer , doi:10.1016/j.ijheatmasstransfer.2011.09.033 (2011a)

Lips, S., Meyer, J. P.: Experimental study of convective condensation in an inclined smooth tube. Part II: Inclination effect on pressure drop and void fraction. International Journal of Heat and Mass Transfer , doi:10.1016/j.ijheatmasstransfer.2011.09.034 (2011b)

Lips, S., Meyer, J. P.: A review of two-phase flow in inclined tubes with specific reference to condensation. International Journal of Multiphase Flow **37**(8), 845 (2011c)

Moreno Quibén, J., Thome, J. R.: Flow pattern based two-phase frictional pressure drop model for horizontal tubes. Part II: New phenomenological model. International Journal of Heat and Fluid Flow **28**(5), 1060 (2007)

Rouhani, S., Axelsson, E.: Calculation of void volume fraction in the subcooled and quality boiling regions. International Journal of Heat and Mass Transfer **13**(2), 383 (1970)

Spedding, P. L., Chen, J. J. J., Nguyen, V. T.: Pressure drop in two phase gas-liquid flow in inclined pipes. International Journal of Multiphase Flow **8**(4), 407 (1982)

Steiner, D.: Heat transfer to boiling saturated liquids. VDI-Wārmeatlas (VDI Heat Atlas), Verein Deutscher Ingenieure, VDI-Gesellschaft Verfahrenstechnik und Chemieingenieurwesen (GCV), Düsseldorf, Chapter Hbb (1993)

Suliman, R., Liebenberg, L., Meyer, J. P.: Improved flow pattern map for accurate prediction of the heat transfer coefficients during condensation of R-134a in smooth horizontal tubes and within the low-mass flux range. International Journal of Heat and Mass Transfer **52**(25-26), 5701 (2009)

Thome, J. R., El Hajal, J., Cavallini, A.: Condensation in horizontal tubes. Part 2: new heat transfer model based on flow regimes. International Journal of Heat and Mass Transfer **46**(18), 3365 (2003)

Wang, W. C., Ma, X. H., Wei, Z. D., Yu, P.: Two-phase flow patterns and transition characteristics for in-tube conden-

sation with different surface inclinations. International Journal of Heat and Mass Transfer **41**(24), 4341 (1998)
Würfel, R., Kreutzer, T., Fratzscher, W.: Turbulence transfer processes in adiabatic and condensing film flow in an inclined tube. Chemical Engineering & Technology **26**(4), 439 (2003)